Monatshefte für Chemie 136, 1985–1991 (2005)
DOI 10.1007/s00706-005-0375-y

Monatshefte für Chemie
Chemical Monthly
Printed in Austria

Syntheses and Structure of $Gd_3Rh_{1.940(7)}In_4$

Ute Ch. Rodewald[1], **Mar'yana Lukachuk**[1,2], **Rolf-Dieter Hoffmann**[1],
and **Rainer Pöttgen**[1,*]

[1] Institut für Anorganische und Analytische Chemie and NRW Graduate School
of Chemistry, Westfälische Wilhelms-Universität Münster, 48149 Münster (Germany)
[2] Max-Plank-Institut für Festkörperforschung, 70569 Stuttgart (Germany)

Received March 24, 2005; accepted April 22, 2005

Summary. The gadolinium–rhodium–indide $Gd_3Rh_{1.940(7)}In_4$ was prepared by arc-melting of the elements and subsequent annealing in a corundum crucible in a sealed silica tube. $Gd_3Rh_{1.940(7)}In_4$ adopts the hexagonal $Lu_3Co_{1.87}In_4$ type, space group $P\bar{6}$, $a = 781.4(5)$, $c = 383.8(3)$ pm, $wR2 = 0.0285$, BASF $= 0.375(1)$ (merohedric twinning *via* a twofold axis (*xx*0)), 648 F^2 values, 22 variables. The structure is derived from the well known ZrNiAl type through an ordering of rhodium and indium atoms on the Ni2 sites. The Rh/In ordering forces a reduction of the space group symmetry from $P\bar{6}2m$ to $P\bar{6}$, leading to merohedric twinning for the investigated crystal. The Rh1 site has an occupancy of only 94.0(7)%. The investigated crystal had a composition $Gd_3Rh_{1.940(7)}In_4$. The main geometrical motif are three types of centered, tricapped trigonal prisms, *i.e.*, $[Rh1In2_6Gd_3]$, $[Rh2Gd_6In2_3]$, and $[In1Gd_6In2_3]$. The shortest interatomic distances occur for Rh–In (276–296 pm) followed by In–In (297 pm). Together, the rhodium and indium atoms build up a three-dimensional $[Rh_{1.940(7)}In_4]$ network, in which the gadolinium atoms fill slightly distorted pentagonal channels. The crystal chemistry of $Gd_3Rh_{1.940(7)}In_4$ is discussed on the basis of a group-subgroup scheme.

Keywords. Gadolinium compounds; Crystal chemistry; Superstructure.

Introduction

The rare earth (*RE*) metal-rhodium–indium systems have intensively been investigated in recent years with respect to phase analysis, crystal chemistry, and physical properties of the respective ternary compounds. So far, more than 50 compounds have been observed in the series RE_2Rh_2In, $RERhIn$, $RE_{10}Rh_{9\pm x}In_{20}$, $RERhIn_2$, $RERhIn_5$, and RE_2RhIn_8 for a variety of rare earth elements. The crystal chemistry and the properties of these intermetallics have recently been reviewed [1, 2]. Also, some $RE_xRh_yIn_z$ compounds occur, which have only one representative within the rare earth series. $YbRhIn_4$ [3] and $EuRh_2In_8$ [4] belong to this class of compounds. They contain divalent ytterbium and europium and consequently they adopt

---

[*] Corresponding author. E-mail: pottgen@uni-muenster.de

another structure type than the compounds with a trivalent rare earth element. With scandium, the smallest rare earth metal, the indide $Sc_3Rh_{1.594(9)}In_4$ [5] is formed. The latter crystallizes with a new superstructure of the $Lu_3Co_{1.87}In_4$ type [6] which results from a puckering effect. Another peculiar compound is $La_{1.18}Rh_3In_2$ [7]. Here, the rhodium and indium atoms build up a rigid three-dimensional network in which the lanthanum atoms fill larger hexagonal channels in a modulated fashion.

Currently we investigated the Gd–*T*–In (*T* = late transition metal) systems in more detail with respect to structure-property relations [8–12]. Such gadolinium based materials may exhibit relatively high magnetic ordering temperatures and they may find application for magnetic refrigeration devices, since they often exhibit enhanced adiabatic temperatures [13–15].

During the phase analytical studies we obtained a hexagonal compound with the tentative composition $Gd_3Rh_2In_4$ with lattice parameters close to those of ZrNiAl type GdRhIn [16, 17]. The higher indium content in $Gd_3Rh_2In_4$, with respect to GdRhIn, led to a larger a and a smaller c lattice parameter. It came out, that $Gd_3Rh_{1.940(7)}In_4$ is isostructural to $Lu_3Co_{1.87}In_4$ [6]. The preparation, structure refinement, and crystal chemistry of this new gadolinium based indide are reported herein.

Discussion

The new indide $Gd_3Rh_{1.94}In_4$ crystallizes with the $Lu_3Co_{1.87}In_4$ structure [6]. This structure type derives from the well known ZrNiAl type [18–20]. As an example we present a projection of the HoRhIn structure [17] onto the *xy* plane in Fig. 1. The 2*c* Rh2 position of HoRhIn splits into two one-fold positions, 1*c* and 1*e* (Fig. 2), that are occupied by the In1 and Rh2 atoms, respectively, in the new gadolinium compound. Thus, the symmetry reduction from $P\bar{6}2m$ to $P\bar{6}$ is caused by a different coloring on that site.

As emphasized in Fig. 1, the overall geometrical motif in this family of intermetallic compounds are tricapped, centered trigonal prisms: $[Rh1In_6Ho_3]$ and

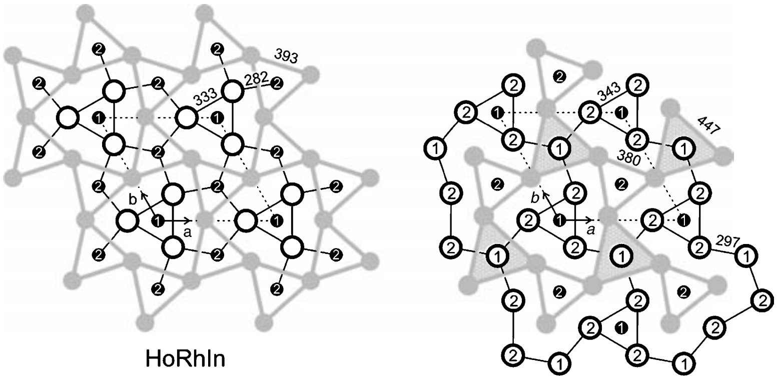

Fig. 1. Projections of the HoRhIn and $Gd_3Rh_{1.940(7)}In_4$ structures onto the *xy* planes; all atoms lie on mirror planes at $z = 0$ (thin lines) and $z = 1/2$ (thick lines); rare earth metal, rhodium, and indium atoms are drawn as gray, filled, and open circles, respectively; some trigonal prismatic building groups and relevant interatomic distances are indicated

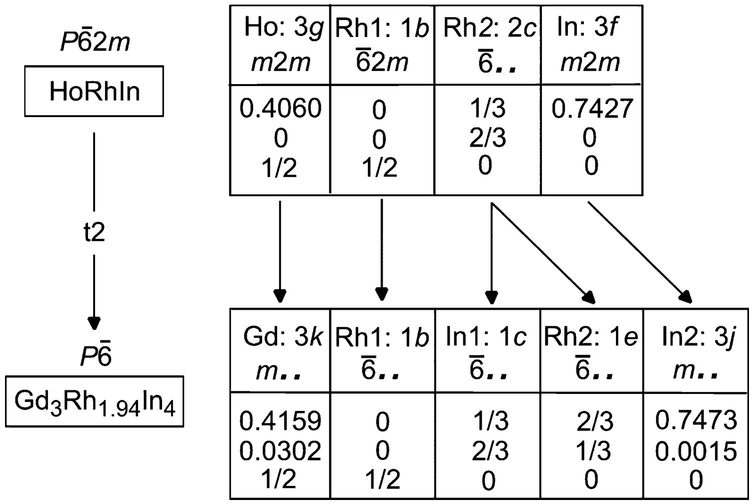

Fig. 2. Group-subgroup scheme in the *Bärnighausen* formalism [28, 29] for the structures of HoRhIn [17] and Gd$_3$Rh$_{1.940(7)}$In$_4$; the evolution of the atomic parameters is shown at the right-hand part; the 1*b* Rh1 site in Gd$_3$Rh$_{1.940(7)}$In$_4$ is occupied by only 94.0(7)%

[Rh2Ho$_6$In$_3$] in HoRhIn and [Rh1In2$_6$Gd$_3$], [Rh2Gd$_6$In2$_3$], and [In1Gd$_6$In2$_3$] in Gd$_3$Rh$_{1.94}$In$_4$. Due to the different coloring of the atoms centering the Gd$_6$ prisms, we observe significant differences in the edge lengths of the triangular basis of the prisms. If an In1 atom centers the prism, the edge length is 447 pm, as compared to 380 pm, if the smaller Rh2 atoms fill such a prism. For comparison, in HoRhIn, where only rhodium atoms center the Ho$_6$ prisms, the Ho–Ho distance is 393 pm.

Due to the In1 atoms centering the Gd$_6$ prisms we observe a different indium substructure in Gd$_3$Rh$_{1.94}$In$_4$. Whereas only In$_3$ triangles with In–In distances of 333 pm occur in HoRhIn, we now observe a two-dimensional indium substructure in Gd$_3$Rh$_{1.94}$In$_4$ with shorter In1–In2 (297 pm) and longer In2–In2 (343 pm) distances. Especially the In1–In2 distances are significantly shorter than the In–In distances in tetragonal body-centered indium (4×325 and 8×338 pm) [21]. With the smaller scandium atoms in Sc$_3$Rh$_{1.594}$In$_4$ one observes even shorter In1–In2 distances of 290 pm.

The two-dimensional indium network is connected in the third direction *via* short Rh1–In2 contacts (276 pm) which are close to the sum of the covalent radii of 275 pm [22]. Also the Rh2 atoms contribute to this network, however, the Rh2–In2 distances of 296 pm are somewhat larger. Together, the rhodium and indium atoms build up a three-dimensional [Rh$_{1.94}$In$_4$] network, in which the gadolinium atoms are located in distorted pentagonal channels. The shortest contact of the gadolinium atoms to the polyanionic network occurs *via* the Gd–Rh2 bonds at 291 pm. For further details on the crystal chemistry and chemical bonding in ZrNiAl related intermetallic compounds we refer to the recent literature [5, 23–25].

Experimental

Synthesis

Starting materials for the preparation of Gd$_3$Rh$_2$In$_4$ were gadolinium ingots (Johnson Matthey), rhodium powder (*ca.* 200 mesh, Degussa-Hüls), and indium tear drops (Heraeus), all with stated purities

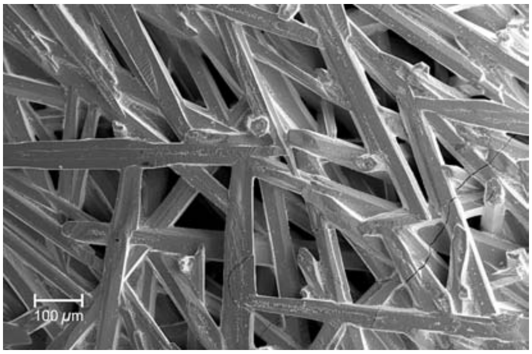

Fig. 3. Scanning electron micrograph of the surface of an arc-molten button of $Gd_3Rh_2In_4$

better than 99.9%. In a first step, pieces of the gadolinium ingot were melted under 600 m bar argon to a small button in an arc-melting furnace [26]. The argon was purified over titanium sponge (900 K), silica gel, and molecular sieves. The pre-melting procedure reduces shattering during the subsequent reaction with rhodium and indium. The gadolinium button was then mixed with a cold-pressed pellet (∅ 6 mm) of rhodium and pieces of the indium tear drops in the ideal 3:2:4 atomic ratio and arc-melted. The product button was remelted three times in order to ensure homogeneity. $Gd_3Rh_{1.940(7)}In_4$ crystallizes directly from the melt. The surface of the arc-molten button was covered with many lath-shaped crystals (Fig. 3). The latter, however, had bad quality for X-ray diffraction.

The button was subsequently placed in a corundum crucible, sealed in an evacuated silica ampoule and first heated within 3 h to 1295 K, kept at that temperature for 3 h, and then cooled at a rate of 5 K/h to 1070 K. In a second step the ampoule was cooled to 770 K at a rate of 15 K/h and finally within 7 h to room temperature. The brittle product (see cracks in Fig. 3) showed no reaction with the container material. The polycrystalline button and small single crystals are light gray with metallic luster. Powders are dark gray. The sample is stable in moist air over months.

Scanning Electron Microscopy

The single crystals investigated on the diffractometer and the bulk sample have been analyzed by EDX measurements using a LEICA 420 I scanning electron microscope with gadolinium trifluoride, rhodium, and indium arsenide as standards. No impurity elements were detected. Various point analyses on the crystals revealed the composition 35 ± 2 at.-% Gd: 21 ± 2 at.-% Rh: 44 ± 2 at.-% In, close to the values obtained from the structure refinement.

X-Ray Film Data and Structure Refinement

The arc-melted and the annealed sample were analyzed through a *Guinier* powder pattern using Cu $K\alpha_1$ radiation and α-quartz ($a = 491.30$, $c = 540.46$ pm) as an internal standard. The *Guinier* camera was equipped with an imaging plate system (Fujifilm BAS-1800). The hexagonal lattice parameters (Table 1) were obtained from a least-squares refinement of the powder data. The correct indexing of the pattern was ensured through an intensity calculation [27] using the atomic positions obtained from the structure refinement. The lattice parameters derived from the single crystal and the powder agree well.

Lath-shaped single crystals of $Gd_3Rh_{1.940(7)}In_4$ were isolated from the annealed sample by mechanical fragmentation and examined by *Laue* photographs on a *Buerger* precession camera (equipped with an imaging plate system, Fujifilm BAS-1800) in order to establish suitability for intensity data collection. Intensity data were recorded at room temperature by use of a *Stoe* IPDS-II image plate diffractometer. A numerical absorption correction was applied to the data. All relevant crystallographic details for the data collection and evaluation are listed in Table 1.

Table 1. Crystal data and structure refinement for $Gd_3Rh_{1.940(7)}In_4$ with $Lu_3Co_{1.87}In_4$ type structure, space group $P\bar{6}$; Z = 1

Empirical formula	$Gd_3Rh_{1.940(7)}In_4$
Molar mass	378.95 g/mol
Unit cell dimensions	$a = 781.4(5)$ pm
(*Guinier* powder)	$c = 383.8$ (3) pm
Calculated density	9.30 g/cm^3
Crystal size	$15 \times 15 \times 35\ \mu m^3$
Detector distance	60 mm
Exposure time	35 min
ω range; increment	0–180°; 1.0°
Integr. param. A, B, EMS	13.5; 3.5; 0.012
Transm. ratio (max/min)	1.81
Absorption coefficient	39.2 mm^{-1}
$F(000)$	478
θ range	3° to 35°
Range in *hkl*	±12, ±12, ±5
Total no. reflections	3068
Independent reflections	648 ($R_{int} = 0.0328$)
Reflections with $I > 2\sigma(I)$	635 ($R_\sigma = 0.0209$)
Data/parameters	648/22
Goodness-of-fit on F^2	1.197
Final R indices [$I > 2\sigma(I)$]	$R1 = 0.0150$
	$wR2 = 0.0284$
R indices (all data)	$R1 = 0.0156$
	$wR2 = 0.0285$
Twin matrix	010 100 00$\bar{1}$
BASF	0.375(1)
Flack parameter	−0.01(2)
Extinction coefficient	0.0021(3)
Largest diff. peak and hole	1.11/−1.20 e/Å^3

The refined hexagonal unit cell parameters and the intensity distribution indicated similarity with the ZrNiAl type structure of GdRhIn [16], space group $P\bar{6}2m$. Refinement of the structure in that space group, assuming the atomic parameters of HoRhIn [17] as starting values revealed an enhanced residual ($R1 \approx 0.12$) and an extremely large U_{22} value for the gadolinium site. Also it turned out that the unit cell of the $Gd_3Rh_{1.940(7)}In_4$ sample shows a larger a and a smaller c parameter as compared to GdRhIn. Furthermore, careful analyses of the diffractometer data set revealed low hexagonal *Laue* symmetry for the $Gd_3Rh_{1.940(7)}In_4$ crystal, similar to the structure of $Lu_3Co_{1.87}In_4$ [6], space group $P\bar{6}$. Thus we observe a *translationengleiche* symmetry reduction of index 2 (t2) from space group $P\bar{6}2m$ to $P\bar{6}$. Consequently we have calculated the atomic parameters for the lower symmetry model, as indicated in the *Bärnighausen* tree [28, 29] in Fig. 2. Subsequent refinement of the structure using SHELXL-97 [30] (full-matrix least-squares on $F_o{}^2$) with anisotropic displacement parameters for all atoms did not drop the residual significantly. Similar to the $Sc_3Ni_{2.10}In_{3.60}$ crystal [5] we observed merohederic twinning due to the *translationengleiche* symmetry reduction of index 2. We have then introduced the twin matrix (010 100 00$\bar{1}$) and refined the structure again, resulting in a twin ratio 62.5/37.5 and a very low weighted residual (see Table 1). Since rhodium and indium differ only by four electrons, the occupancy parameters were refined in a separate series of least-squares cycles. The Gd, Rh2, In1, and In2 sites were fully occupied within one standard deviation, while the Rh1

Table 2. Atomic coordinates and isotropic displacement parameters (pm^2) of $Gd_3Rh_{1.940(7)}In_4$; U_{eq} is defined as one third of the trace of the orthogonalized U_{ij} tensor; the anisotropic displacement factor exponent takes the form $-2\pi^2[(ha^*)^2U_{11} + \cdots + 2kha^*b^*U_{12}]$; $U_{13} = U_{23} = 0$

Atom	*Wyck.*	Occ.	*x*	*y*	*z*	U_{11}	U_{22}	U_{33}	U_{12}	U_{eq}
Gd	3*k*	1.00	0.41594 (7)	0.03017 (5)	1/2	134 (2)	106 (2)	94 (1)	55 (1)	114 (1)
Rh1	1*b*	0.940 (7)	0	0	1/2	111 (4)	U_{11}	212 (7)	55 (2)	144 (4)
Rh2	1*e*	1.00	2/3	1/3	0	103 (3)	U_{11}	84 (6)	52 (1)	97 (2)
In1	1*c*	1.00	1/3	2/3	0	84 (3)	U_{11}	202 (6)	42 (1)	123 (2)
In2	3*j*	1.00	0.74729 (8)	0.0015 (1)	0	126 (3)	98 (2)	199 (3)	49 (2)	144 (1)

Table 3. Interatomic distances (pm) of $Gd_3Rh_{1.940(7)}In_4$, calculated with the powder lattice parameters; standard deviations are all equal or less than 0.3 pm; all distances within the first coordination spheres are listed

Gd:	2	Rh2	291.4	In1:	3	In2	297.4
	1	Rh1	313.9		6	Gd	321.5
	2	In1	321.5	In2:	2	Rh1	275.8
	2	In2	324.1		1	Rh2	295.9
	2	In2	331.9		1	In1	297.4
	2	In2	346.6		2	Gd	324.1
	2	Gd	379.8		2	Gd	331.9
	2	Gd	383.8		2	In2	343.0
Rh1:	6	In2	275.8		2	Gd	346.6
	3	Gd	313.9				
Rh2:	6	Gd	291.4				
	3	In2	295.9				

site shows small defects, similar to $Sc_3Rh_{1.594}In_4$ [5] and $Lu_3Co_{1.87}In_4$ [6]. Thus, the occupancy parameter of Rh1 was refined as a least-squares variable in the final cycles. Refinement of the correct absolute structure was ensured through refinement of the *Flack* parameter [31, 32]. A final difference *Fourier* synthesis was flat. The refined atomic parameters and interatomic distances are listed in Tables 2 and 3. Further details on the structure refinement may be obtained from Fachinformationszentrum Karlsruhe, D-76344 Eggenstein-Leopoldshafen (Germany), by quoting the Registry No. CSD-415252.

As is evident from Table 2, the Rh1, In1, and In2 atoms show a U_{33} displacement parameter that is about two times larger than the U_{11} and U_{22} parameter. This might be indicative for a violation of the mirror planes perpendicular to the *c* axis, similar to the structure of $Sc_3Rh_{1.594}In_4$ [5], where a doubling of the *c* parameter was observed. Careful examination of the image plate data set, however, did not reveal additional reflections, nor diffuse scattering in the *c* direction.

Acknowledgements

We thank *H.-J. Göcke* for the work at the scanning electron microscope. This work was supported by the Deutsche Forschungsgemeinschaft through the priority program SPP 1166 *Lanthanoidspezifische Funktionalitäten in Molekül und Material*. *M.L.* is indebted to the NRW Graduate School of Chemistry for a PhD stipend.

References

[1] Kalychak YaM, Zaremba VI, Pöttgen R, Lukachuk M, Hoffmann R-D (2005) Rare Earth-Transition Metal-Indides. In: Gschneidner KA Jr, Pecharsky VK, Bünzli JC (eds) Handbook on the Physics and Chemistry of Rare Earths. Elsevier, Amsterdam, vol 34, chapt 218

[2] Lukachuk M, Rodewald UCh, Zaremba VI, Hoffmann RD, Pöttgen R (2004) Z Anorg Allg Chem **630**: 2253

[3] Hoffmann R-D, Pöttgen R, Zaremba VI, Kalychak YaM (2000) Z Naturforsch **55b**: 834

[4] Kußmann D, Pöttgen R (2001) Z Anorg Allg Chem **627**: 55

[5] Lukachuk M, Zaremba VI, Hoffmann R-D, Pöttgen R (2004) Z Naturforsch **59b**: 182

[6] Zaremba VI, Kalychak YaM, Zavalii PYu, Sobolev AN (1989) Dopov Akad Nauk Ukr RSR Ser B 38

[7] Esmaeilzadeh S, Zaremba VI, Kalychak YaM, Hoffmann R-D, Pöttgen R (2002) Solid State Sci **4**: 93

[8] Pöttgen R, Kotzyba G, Görlich EA, Latka K, Dronskowski R (1998) J Solid State Chem **141**: 352

[9] Łątka K, Kmieć R, Rams M, Pacyna AW, Zaremba VI, Pöttgen R (2004) Z Naturforsch **59b**: 947

[10] Zaremba VI, Hlukhyy V, Pöttgen R (2005) Z Anorg Allg Chem **631**: 327

[11] Łątka K, Kmieć R, Rams M, Pacyna AW, Zaremba VI, Rodewald UCh, Pöttgen R (2005) Solid State Sci (submitted)

[12] Łątka K, Lukachuk M, Pöttgen R (2005) (unpublished results)

[13] Pecharsky VK, Gschneidner KA Jr (1997) Appl Phys Lett **70**: 3299

[14] Pecharsky VK, Gschneidner KA Jr (1998) Adv Cryog Eng **43**: 1729

[15] Gschneidner Jr KA, Pecharsky VK (2000) Annu Rev Mater Sci **30**: 387

[16] Ferro R, Marazza R, Rambaldi G (1974) Z Anorg Allg Chem **410**: 219

[17] Lukachuk M, Zaremba VI, Pöttgen R (2003) Intermetallics **11**: 581

[18] Krypyakevich PI, Markiv VYa, Melnyk EV (1967) Dopov Akad Nauk Ukr RSR Ser A 750

[19] Dwight AE, Mueller MH, Conner RA Jr, Downey JW, Knott H (1968) Trans Met Soc AIME **242**: 2075

[20] Zumdick MF, Hoffmann R-D, Pöttgen R (1999) Z Naturforsch B **54**: 45

[21] Donohue J (1974) The Structures of the Elements. Wiley, New York

[22] Emsley J (1999) The Elements. Oxford University Press, Oxford

[23] Zhao JT, Parthé E (1990) Acta Crystallogr C **46**: 2273

[24] Parthé E, Gelato L, Chabot B, Penzo M, Cenzual K, Gladyshevskyy R (1993) TYPIX – Standardized data and crystal chemical characterization of inorganic structure types. Gmelin Handbook of inorganic and organometallic chemistry, 8th ed. Springer, Berlin

[25] Zumdick MF, Pöttgen R (1999) Z Kristallogr **214**: 90

[26] Pöttgen R, Gulden Th, Simon A (1999) GIT Labor Fachzeitschrift **43**: 133

[27] Yvon K, Jeitschko W, Parthé E (1977) J Appl Crystallogr **10**: 73

[28] Bärnighausen H (1980) Commun Math Chem **9**: 139

[29] Bärnighausen H, Müller U (1996) Symmetriebeziehungen zwischen den Raumgruppen als Hilfsmittel zur straffen Darstellung von Strukturzusammenhängen in der Kristallchemie. University of Karlsruhe and University GH Kassel

[30] Sheldrick GM (1997) SHELXL-97, Program for Crystal Structure Refinement, University of Göttingen

[31] Flack HD, Bernadinelli G (1999) Acta Crystallogr A **55**: 908

[32] Flack HD, Bernadinelli G (2000) J Appl Crystallogr **33**: 1143